Spectroscopic Demonstration of Exciton Dynamics and Excimer Formation in a Sterically Controlled Perylene Bisimide Dimer Aggregate

ARTICLE *in* JOURNAL OF PHYSICAL CHEMISTRY LETTERS · OCTOBER 2014

Impact Factor: 7.46 · DOI: 10.1021/jz501953a

THE JOURNAL OF PHYSICAL CHEMISTRY Letters

Letter

pubs.acs.org/JPCL

Spectroscopic Demonstration of Exciton Dynamics and Excimer Formation in a Sterically Controlled Perylene Bisimide Dimer Aggregate

Minjung Son,[†] Kyu Hyung Park,[†] Changzhun Shao,[‡] Frank Würthner,*[,‡] and Dongho Kim*[,†]

[†]Spectroscopy Laboratory for Functional π-Electronic Systems and Department of Chemistry, Yonsei University, Seoul 120-749, Korea

[‡]Institut für Organische Chemie and Center for Nanosystems Chemistry, Universität Würzburg, Am Hubland, 97074 Würzburg, Germany

Supporting Information

ABSTRACT: Although it is commonly known that H-type PBI aggregates give rise to a broad, red-shifted excimer fluorescence with considerably longer fluorescence lifetimes than observed for the monomers, the underlying mechanisms of excimer formation and other relevant exciton dynamics in such π-stacked systems are still far from being understood. In this context, we demonstrate a thorough spectroscopic investigation on the exciton relaxation pathways, including excimer formation, in a perylene-3,4:9,10-bis(dicarboximide) (PBI) dimer aggregate **1** by using time-resolved fluorescence and transient absorption spectroscopy combined with excitation-power and polarization dependence. It was found that the excited dimer formation process followed by structural rearrangement is approximately two times faster than observed within larger PBI aggregates. Excitation-power-dependent transient absorption decay profiles revealed the fully delocalized nature of excitons in the dimer as opposed to larger stacks.

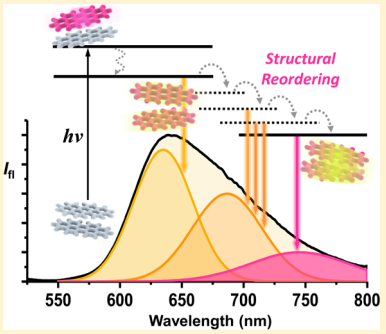

SECTION: Spectroscopy, Photochemistry, and Excited States

Molecular aggregates composed of π-conjugated molecular systems have recently drawn tremendous attention as their functional properties and the electronic interactions between building blocks can easily be modulated by varying the temperature, solvent polarity, and concentration.[1−4] Moreover, because the noncovalent nature of the driving force of aggregation, that is, π−π stacking, allows a variety of different morphologies to arise from a given monomer unit,[5−8] these systems are considered promising platforms for evaluating and controlling structure-dependent intermolecular interactions between the functional units.

Inspired by their excellent aggregating property in concentrated solution phase as well as outstanding photostability and high fluorescence quantum yields,[9] a myriad of fascinating examples of aggregates based on 3,4,9,10-perylene tetracarboxylic acid bisimides (PBIs) have been reported.[2,4,9] However, size-selective formation of excimers, that is, excited dimers or multimers, relaxation behaviors and the interactions between excitons in π-stacked PBIs remains to date largely unexplored. Although there were several attempts from theory to unravel the nature of excitons in a generic PBI H-aggregate by simulating their steady-state absorption and emission features by quantum chemical and dynamical calculations,[10−12] the results still overlook the potential subtle alteration in their exciton behaviors by the presence of additional surrounding chromophores as the aggregate grows larger, suggesting that dimers and extended aggregates should behave exactly the same in the excited state.

In this context, in contrast to previous PBI monomers that self-assemble into mixtures of small-sized oligomers, we recently prepared a novel bay-unsubstituted PBI **1** (Figure 1a) that only forms noncovalent dimer assembly by π−π stacking but does not proceed to further aggregation in the binary solvent mixture (v:v = 1:5) of $CHCl_3$ and methylcyclohexane (MCH) due to the steric encumbrance originating from the presence of bulky 2,5-di-*tert*-butylphenyl substituents at one of the two imide positions.[13] Furthermore, in light of its tunable aggregation behavior driven by solvophobic effect,[14,15] which affords further aggregation of **1** into larger aggregates in pure MCH, we have comparatively analyzed the two extreme modes of stacked **1** with respect to their excited-state behaviors. The exclusively formed dimer, the simplest and most fundamental unit of molecular aggregate, in $CHCl_3$/MCH solvent system, serves as an ideal starting point for elucidation of the complex photodynamic nature of even larger PBI aggregates. Although differentiation between PBI stacks of different sizes could only ambiguously and indirectly be achieved by NMR spectroscopy or calculation, herein, we report for the first time a comprehensive spectroscopic

Received: September 15, 2014
Accepted: October 3, 2014

   dx.doi.org/10.1021/jz501953a | J. Phys. Chem. Lett. 2014, 5, 3601−3607

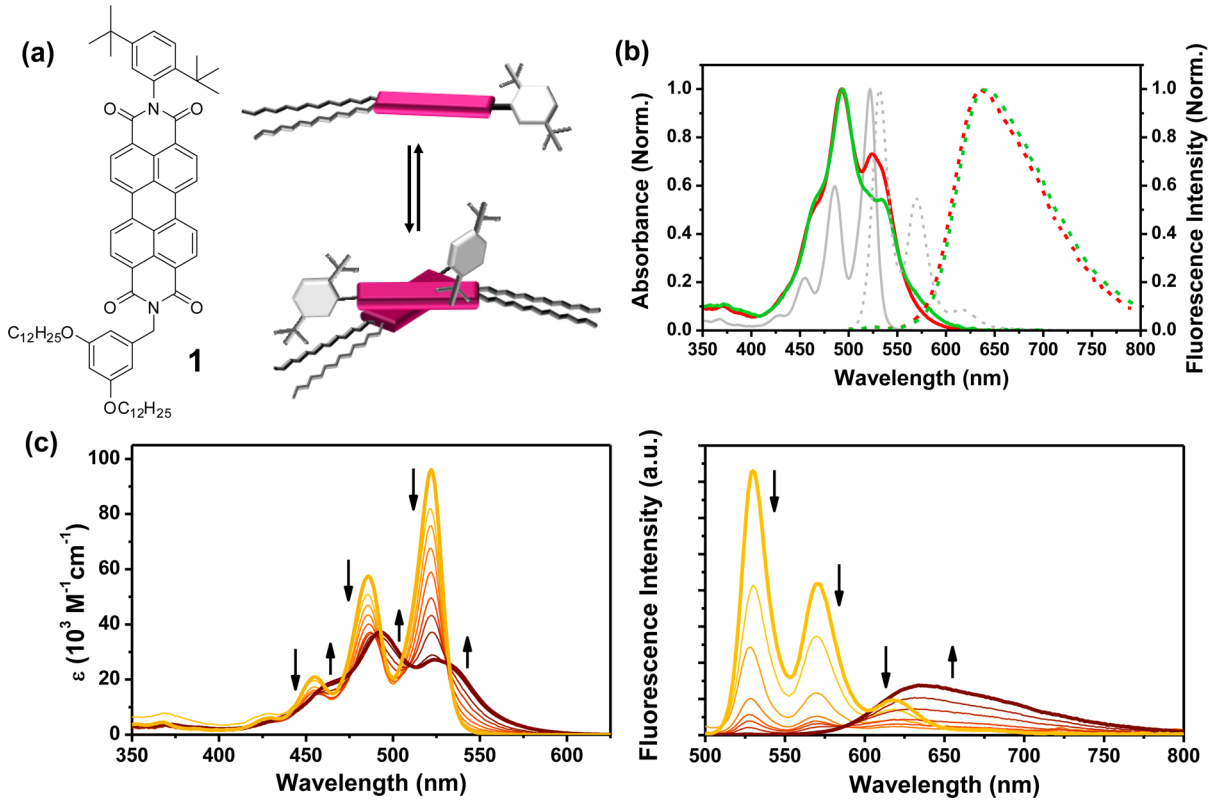

Figure 1. (a) Molecular structure of **1** (left) and schematic representation of the dimerization process (right). (b) Steady-state absorption (solid lines) and fluorescence emission (dashed lines) spectra of **1** in $CHCl_3$/MCH (v:v = 1:5; red) and pure MCH (green). The molar concentration employed is 1.25×10^{-2} M. Absorption and emission of **1** in dilute condition ($<10^{-6}$ M) are indicated in gray shade for comparison. (c) Concentration-dependent UV/vis absorption (left) and fluorescence emission spectra (right; λ_{exc} = 480 nm) of **1** in $CHCl_3$/MCH (v:v = 1:5) in the concentration range from 1.25×10^{-5} (yellow) to 1.25×10^{-2} M (dark brown).

Table 1. Absorption and Emission Maxima, λ_{abs} and λ_{emi}, Fluorescence Quantum Yields, Φ_{fl}, 0−0/0−1 absorption peak ratio, A_{0-0}/A_{0-1}, Splitting Values, $\Delta\nu$, and Fluorescence Lifetimes, τ_{fl}, of 1 Measured in $CHCl_3$/MCH[a] and MCH at Different Molar Concentrations

solvent		λ_{abs} (nm)	λ_{emi} (nm)	Φ_{fl}	A_{0-0}/A_{0-1}	$\Delta\nu$ (eV)	τ_{fl} (ns)
$CHCl_3$/MCH (v:v = 1:5)	dil.[b]	455, 486, 522	528, 570, 618	0.21	1.65	0.18	1.6 (monomer)
	conc.[b]	460 (sh.[c]), 493, 524	526, 634	0.008	0.73	0.14	17 (dimer)
MCH	dil.[b]	452, 482, 518	524, 563, 609	0.82	1.64	0.18	3.5 (monomer)
	conc.[b]	462 (sh.[c]), 494, 537	525, 639	0.09	0.54	0.21	30 (aggregate)

[a]Ratio is v:v = 1:5. [b]Where dil. (dilute) = 1.25×10^{-5} M, conc. (concentrated) = 1.25×10^{-2} M. [c]Shoulder peaks.

demonstration of clearly different exciton behaviors in a dimer and a larger PBI aggregate formed from the same monomer building block. Size-dependent excimer formation, structural reordering dynamics and exciton relaxation pathways were revealed by various time-resolved spectroscopic techniques along with polarization- and excitation-power dependent measurements.

The steady-state absorption and fluorescence emission spectra of **1** were measured at room temperature by varying the molar concentration from 1.25×10^{-5} M, in which only monomers prevail, to 1.25×10^{-2} M, where the predominant form of the molecules is the stacked dimer.[13] Clear concentration dependence revealed in the absorption and emission spectra (Figure 1b,c) suggests the formation of aggregates by intermolecular $\pi-\pi$ interaction.

The absorption and fluorescence spectra display characteristic spectral features of a helically stacked PBI aggregate. As opposed to a PBI monomer, whose absorption and emission spectra are easily recognized by well-resolved vibronic progression of the S_0-S_1 transition,[16] at higher (above millimolar) concentrations the 0−0 absorption band gets gradually diminished, leading to the reversal of 0−0 and 0−1 band intensities. This distinctive spectral feature well reflects the excitonic nature of an H-aggregate where the lower Frenkel exciton state is forbidden.[17,18] Monomer fluorescence is also replaced by a broad and structureless excimer emission band peaking at 634 nm, accompanied by several isosbestic points indicating the equilibrium between exclusively two species (monomer and dimer). Meanwhile, it was hardly possible to distinguish between the dimer and a larger aggregate merely by comparing their steady-state spectra (Supporting Information Figure S1). Still, it could be derived from two parameters—the intensity ratio (A_{0-0}/A_{0-1}) and the splitting ($\Delta\nu$) of 0−0 and 0−1 bands—that different aggregate species are present in each solvent (Table 1). In a previous work by Seibt et al.,[10] it was revealed by introducing dimer Hamiltonian[19,20] that these two

dx.doi.org/10.1021/jz501953a | J. Phys. Chem. Lett. 2014, 5, 3601−3607

parameters are strongly dependent on the mutual arrangement between the PBI units, as expressed in eqs 1−2

$$J(R, \beta, \alpha_1, \alpha_2) = \frac{d^2}{R^3}[\cos(\beta) - 3\cos(\alpha_1)\cos(\alpha_2)] \quad (1)$$

$$\frac{A_{0-0}}{A_{0-1}} = \left(\frac{\cos(\beta/2)}{\sin(\beta/2)}\right)^2 \quad (2)$$

where J is the coupling element, R is the monomer−monomer separation, d is the magnitude of transition dipole moment, α_1 and α_2 are the angles between the monomer−monomer center-of-mass vector and monomer transition dipole moment, respectively, and β is the azimuth angle between monomer transition dipole moments.

Previous molecular modeling studies using MM3* geometry optimization revealed a rotational displacement (β) of 26° in the dimer, which essentially results in different band structures from those of an extended aggregate with $\beta = 30°$ at its ground-state energy minimum.[11,13] The trends observed in these two parameters under different aggregation regime were strikingly similar to those observed in our previous work that involves a bay-substituted core-distorted dimer stack **2** and a columnar H-type aggregate **3** (Supporting Information Figure S2 and Table S1).[21]

Concentration-dependent time-resolved fluorescence measurements (Table 1 and Supporting Information Figure S3) exhibited double exponential decay profiles with increasing amplitude of excimer fluorescence as the concentration was increased when the excimer emission band (675 nm) was directly monitored. The excimer fluorescence lifetime (17 ns) appeared nearly 10 times longer than that of monomer fluorescence (1.6 ns[22]) due to the preceding vibrational relaxation process toward $\beta = 0°$ on the potential curve where the excimer fluoresces, as suggested by theory.[11]

In a rotationally displaced molecular aggregate like ours, polarization-dependent spectroscopic techniques serve as a powerful tool for unveiling the interaction between excitons with respect to the orientation of transition dipoles.[23,24] In this view, we have monitored the anisotropy decay dynamics of **1** by time-resolved fluorescence anisotropy and transient absorption (TA) anisotropy measurements. A sharply contrasting feature was observed in the fluorescence anisotropy decay profiles of **1** monitored at the monomer (535 nm) and excimer fluorescence band (625 nm), respectively, by varying the concentration (5×10^{-6} to 1.25×10^{-2} M; see Supporting Information Figures S5−S6). Fluorescence anisotropy decay profiles at 535 nm were insensitive to concentration, where the initial anisotropy values ($r_0 \sim 0.35$) at all concentrations approached 0.4, the maximum possible anisotropy value in the absence of any depolarization pathways.[25] On the contrary, when the excimer fluorescence band was directly probed, appreciable interaction between rotationally displaced transition dipoles as well as possible exciton migration therein[21] led to a considerable decrease in r_0 values from 0.34 down to 0.08. It is worth noting that further growth of the aggregate results in an even more significant drop in the r_0 values (inset in Figure 2a) because the nonparallel distribution of the transition dipoles in the larger aggregate eventually leads to an apparent canceling out of the emitting dipole vectors. In the dimer aggregate, on the contrary, only two transition dipoles are in close contact with each other, leading to a significantly less pronounced decrease in the r_0 values with increasing molar concentration. Even in 5 mM,

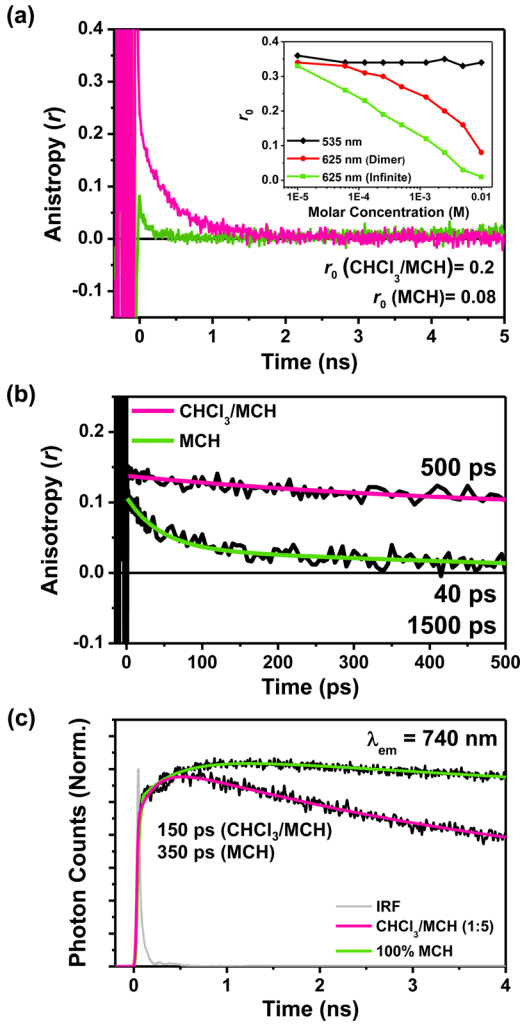

Figure 2. (a) Fluorescence anisotropy decay profiles of **1** ($c = 2.5 \times 10^{-3}$ M) in 1:5 $CHCl_3$/MCH (magenta) and MCH (green) probed at 625 nm under photoexcitation at 450 nm. The initial anisotropy values (r_0) are indicated inside the figure. Inset: Plots of r_0 against molar concentration at 535 (black) and 625 nm (red, in 1:5 $CHCl_3$/MCH; green, in MCH). (b) Femtosecond transient absorption anisotropy decay profiles of **1** ($c = 5 \times 10^{-3}$ M) at the probe wavelength of 710 nm (λ_{pump} = 530 nm) in 1:5 $CHCl_3$/MCH (magenta fitted line) and MCH (green fitted line). (c) Fluorescence decay profiles of **1** ($c = 5 \times 10^{-3}$ M) in 1:5 $CHCl_3$/MCH (magenta fitted line) and MCH (green fitted line) probed at 740 nm under photoexcitation at 450 nm. The instrumental response function (IRF) is represented in gray trace.

where approximately 80% of the molecules are aggregated,[13] r_0 of the dimer was found to be 0.16, whereas that of the larger stack was hardly distinguishable from zero (0.03).

The fitted anisotropy decay times, which correspond to rotational reorientation times of the molecules being probed,[25] were determined to be 550 ps in $CHCl_3$/MCH, resulting in the hydrodynamic diameter of 1.8 nm based on the Perrin equation assuming a spherical fluorophore (eqs 3−4)[25]

$$D_r = \frac{RT}{6V\eta} \quad (3)$$

$$\tau_r = \frac{1}{6D_r} \quad (4)$$

dx.doi.org/10.1021/jz501953a | J. Phys. Chem. Lett. 2014, 5, 3601−3607

Scheme 1. Schematic representation of proposed exciton dynamics in the dimer aggregate 1

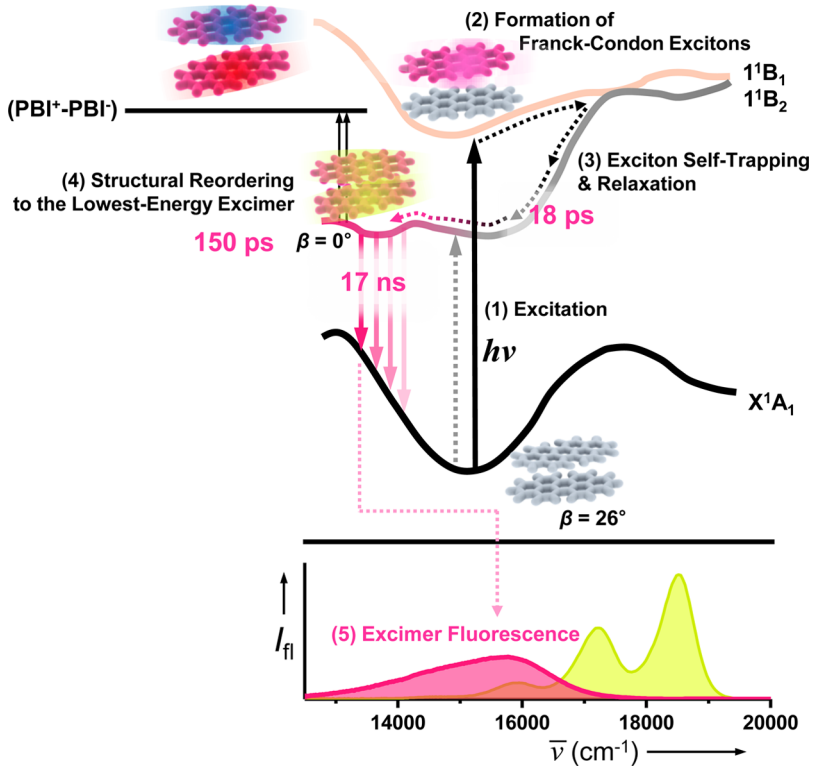

where D_r is the diffusion coefficient, R is the gas constant, T is the temperature in Kelvin, V is the hydrodynamic volume, η is viscosity, and τ_r is the rotational diffusion time.

Comparison of the derived hydrodynamic diameter of nonaggregated **1** (1.8 nm) with that of the dimer aggregate extracted from the DOSY spectrum analysis[13] (3.2 nm) substantiates our dimerization regime. A longer rotational diffusion time (1500 ps) was observed in pure MCH, corroborating the growth of the dimers into larger aggregates, although an accurate determination of the spatial dimension of these aggregates was not possible due to the rigorously reduced quantum yield of excimer fluorescence as well as their nonspherical structures.

Moving further, we have focused our attention on the observation of ultrafast depolarization channels in aggregated **1** within the first few hundred picoseconds, the presence of which was already speculated from the conspicuously decreased (initial) anisotropy values in both steady-state and time-dependent fluorescence anisotropy profiles (Supporting Information Figures S5−S7). Interestingly, transient absorption anisotropy decay profiles probed in the excited-state absorption (ESA) peak (710 nm) of **1** were strongly dependent on the solvent composition, that is, the size of the aggregate (Figure 2b). Although the anisotropy decayed monoexponentially for the dimer aggregate of **1** simply reflecting the rotational diffusion time of 500 ps, an additional component with a time constant of 40 ps was observed in larger aggregates, which is in compliance with our previous work on **2** and **3** (Supporting Information Figure S8).[21] We attribute this depolarization dynamics to the interactions between the rotationally displaced transition dipoles to form the nascent Franck−Condon excitons of the molecular aggregate and their possible migrations within the congregated stacks. The absence of this component in the dimer as well as a higher initial anisotropy value (0.15) compared to the larger aggregate (0.1) likely originate from less pronounced interactions between the two PBI units than in a multichromophoric aggregate composed of more than three PBI molecules, in which the nature of exciton behaviors should be relatively complicated due to additional interactions with other nearby PBI units.

In order to gain insight into the excimer formation dynamics which is closely associated with the aforementioned broad fluorescence band and significantly increased fluorescence lifetime, we have turned our attention to the first few nanoseconds of the time-resolved fluorescence profiles (Figure 2c). When the red edge (740 nm) of excimer fluorescence was monitored for the dimer aggregate of **1**, a clear rise profile was manifested with a time constant of 150 ps, which was moderately shorter than that of the larger aggregate case (350 ps), followed by long excimer fluorescence lifetime. Observation of such rise components, which were not observed in monomers (Supporting Information Figure S9), is the spectroscopic verification of former suggestions by Engel and Engels as well as others that the emitting excimer state is accessed via a structural rearrangement process following the vertical excitation to the singlet exciton state.[18,21,26,27] In other words, upon photoexcitation, the initially formed heterogeneous excimer species undergo a geometry reordering process to approach the lowest-energy excimer state with reduced $\pi-\pi$ distances between PBI planes ((4) in Scheme 1). Here, again, the difference in the fitted time constants is closely associated with differing number of constituent chromophores; because additional interactions with peripheral PBI units are absent in a dimer aggregate, the stacked dimer needs a shorter time for this reordering process than an extended aggregate, in which the spatial arrangement of a greater number of chromophores must be adjusted to reach the most stable excimer state.

dx.doi.org/10.1021/jz501953a | J. Phys. Chem. Lett. 2014, 5, 3601−3607

Combined with analysis of the time evolution of the excimer fluorescence, decomposition of the steady-state fluorescence spectra by Gaussian fitting further supports the presence of such dynamics. Gao et al. reported the simulated fluorescence spectrum of a similarly displaced PBI dimer H-aggregate, which was deconvolved into a higher-energy emission band coming from the initially excited Franck−Condon state and a lower-energy one from the mixed contribution of the structurally rearranged excimer and charge transfer exciton states.[26] Congruently, Gaussian fits to the steady-state fluorescence spectra of **1** required three components to reproduce the experimentally observed fluorescence spectra in both the dimer and the longer aggregate cases (Supporting Information Figure S10), in which the latter two bands are ascribable to the retarded fluorescence originating from the low-lying excimer state following the rearrangement process. In this view, it is evident that our previous observation of the 150−350 ps rise components in time-resolved fluorescence is a consequence of the population transfer from the unrelaxed emitting state (component 1 in Supporting Information Figure S10) to the relaxed "excimer" state (components 2−3 in Supporting Information Figure S10) accompanied by gradual spectral shifts, albeit a corresponding decay profile of the former state was not found, which is likely to be masked by strong monomer fluorescence.[28] Though further aggregation did not affect the overall shape of the fluorescence spectra of **1** (Figure 1b), the reference compound **3** displayed a much intensified second band at 670−700 nm as compared to **1** due to a different ground-state geometry (β = 55°)[18] because the rearrangement process would involve not only alteration of the π−π distances but also shift in the rotational angles (β).

In addition to our previous findings, monitoring of transient absorption (TA) spectra at near-infrared (NIR) region provides us with a straightforward evidence of the excimer formation dynamics of **1**. NIR-TA is especially useful for tracking exclusively the spectral signatures of excimers because the strong $S_1 \rightarrow S_n$ ESA signals do not interfere with pure excimer transitions.[28−30] Wasielewski et al. showed in a recent work that the transition of the excimer to the ion pair state (^{1}*(PBI−PBI) → ^{1}(PBI$^+$−PBI$^-$)) appears as an ESA band peaking at 1550−1770 nm (0.70−0.80 eV).[30] Concentration-dependent NIR-TA spectra (Supporting Information Figure S11) revealed rising ESA bands only for the stacked structures of **1** at 1300−1600 nm but not for the monomer, although their peak positions could not be determined due to the detection limit of our spectrometer (∼1700 nm). As opposed to the monomer that showed a fast decay component due to its aforementioned charge transfer character,[22] kinetic traces of the dimer and the larger aggregate of **1** were all fitted into a monoexponential rise function with the time constants of 18 and 40 ps, respectively (Supporting Information Figure S12), the latter of which was also observed in the TA anisotropy decay of the larger aggregate. Here, each rise component can be attributed to the early stages of excited dimer and multimer formation process accompanied by vibrational relaxation along the potential energy curves as well as exciton self-trapping ((3) in Scheme 1), after which the unrelaxed aggregates can be excited to the ion pair state in NIR region. It should be noted that the time scale of such processes in the dimer aggregate (18 ps) could be exclusively determined by NIR-TA, which was not visible in the TA anisotropy decay profile (Figure 2b).

To evaluate whether the nascent excitons are able to migrate along the stacks before formation of excimer traps, we have performed TA measurements by changing the excitation laser power because excitation with high laser fluence could lead to generation of multiple excitons which results in fast deactivation by their collisional quenching, that is, the exciton−exciton annihilation (EEA) process.[31−33] The transient species of stacked **1** (Figure 3) exhibit broad ground-state

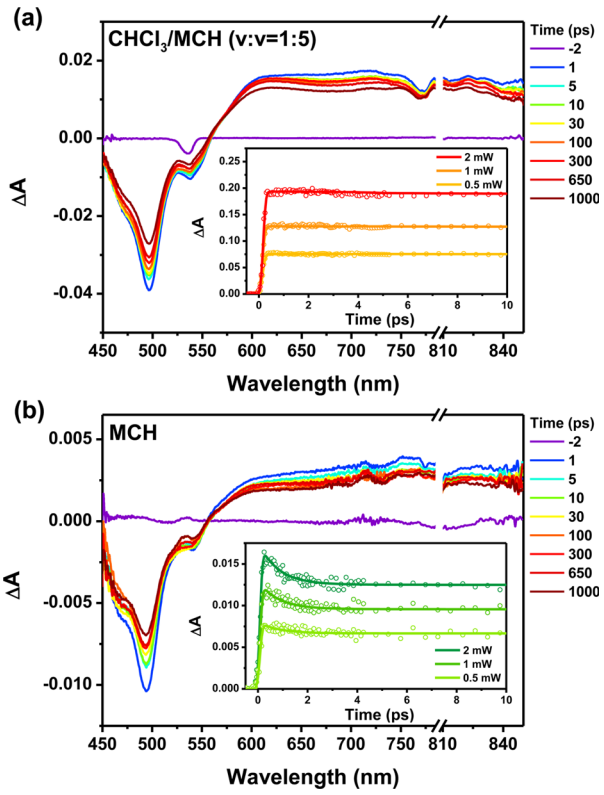

Figure 3. Femtosecond transient absorption spectra of **1** in (a) $CHCl_3$/MCH (v:v = 1:5) and (b) MCH at the molar concentration of 5×10^{-3} M. Insets: Pump-power dependent transient absorption decay profiles under the pump beam intensities of 0.5−2 mW (0.1−0.4 W/cm^2). The pump and probe wavelengths employed are 530 and 825 nm, respectively.

bleaching (GSB) signals up to ∼570 nm and broad featureless excited-state absorption (ESA) from ∼570 nm onward, as opposed to the monomer (Supporting Information Figure S13), whose TA spectra show rather strong stimulated emission (SE) bands at 530−630 nm and much sharper ESA signals peaking at ∼710 nm. Interestingly, whereas the TA spectra of the two aggregate species of **1** could not be distinguished by their spectral features, their kinetic traces revealed great difference from each other. Though the dimer aggregate of **1** did not reveal any power dependence, the extended aggregate showed a prominent pump-power-dependent decay profile with an EEA time of 0.8 ps (insets in Figure 3), which is in excellent agreement with our previous results on dimer stack **2** and longer aggregate **3**.[21] From this size-dependent contrasting behavior, we can conjecture that the noncovalent dimer is subject to complete exciton delocalization between the two PBI units, rendering it to be regarded as a single quantum system. On the other hand, in the larger aggregate, no complete exciton delocalization is achieved, and hence, localized exciton subunits migrate within the aggregate on an ultrafast time scale preceding trapping to the excimer state. We have previously reported that the exciton diffusion length of aggregated **3** is in

dx.doi.org/10.1021/jz501953a | J. Phys. Chem. Lett. 2014, 5, 3601−3607

the range of 5−10 PBI units,[21] which is nevertheless a rough estimation and, thus, needs to be clarified further in future work.

In this work, we have comparatively characterized the excimer formation and exciton relaxation dynamics of PBI dimer aggregates (Scheme 1) that feature solvent-driven switching in the aggregation behavior. Although we only report here the two limiting cases of size-dependent exciton dynamics in PBI aggregates, our findings from time-dependent fluorescence, absorption, and anisotropy provide the most straightforward evidence on the essentially different nature of excitons in a dimer and an infinite aggregate regime, which is expected to overcome the ambiguity addressed by ground-state features and computation. We believe that our results will provide some fundamental insights into further investigation of similar small-sized self-assemblies along with theoretical methods, which will serve as a doorway toward elucidation of the exciton behaviors of more complex molecular aggregates. This work takes a step further from our recent preliminary report[21] on larger aggregates that a direct comparison was provided between two different supramolecular structures constructed out of an identical PBI building block. Our future work will involve realization of a series of size-defined oligomers and systematic exploration on their size-dependent exciton relaxation dynamics.

■ ASSOCIATED CONTENT

Supporting Information

Experimental details, further information on reference compounds **2** and **3**, additional results on steady-state absorption, fluorescence, anisotropy, and time-resolved fluorescence, transient absorption, and time-resolved anisotropy. This material is available free of charge via the Internet at http://pubs.acs.org.

■ AUTHOR INFORMATION

Corresponding Authors

*E-mail: dongho@yonsei.ac.kr.

*E-mail: wuerthner@chemie.uni-wuerzburg.de.

Notes

The authors declare no competing financial interest.

■ ACKNOWLEDGMENTS

The work at Yonsei was financially supported by the Midcareer Researcher Program (2005-0093839) administered through the National Research Foundation of Korea (NRF) funded by the Ministry of Education, Science and Technology (MEST). The researchers from Würzburg are grateful to the Deutsche Forschungsgemeinschaft for financial support of their work within the research graduate school GK 1221 "Control of electronic properties of aggregates of π-conjugated molecules".

■ REFERENCES

(1) Hoeben, F. J. M.; Jonkheijm, P.; Meijer, E. W.; Schenning, A. P. H. J. About Supramolecular Assemblies of π-Conjugated Systems. *Chem. Rev.* **2005**, *105*, 1491−1546.

(2) Wasielewski, M. R. Self-Assembly Strategies for Integrating Light Harvesting and Charge Separation in Artificial Photosynthetic Systems. *Acc. Chem. Res.* **2009**, *42*, 1910−1921.

(3) Shirakawa, M.; Kawano, S.; Fujita, N.; Sada, K.; Shinkai, S. Hydrogen-Bond-Assisted Control of H versus J Aggregation Mode of Porphyrins Stacks in an Organogel System. *J. Org. Chem.* **2003**, *68*, 5037−5044.

(4) Chen, Z.; Lohr, A.; Saha-Möller, C. R.; Würthner, F. Self-Assembled π-Stacks of Functional Dyes in Solution: Structural and Thermodynamic Features. *Chem. Soc. Rev.* **2009**, *38*, 564−584.

(5) Fennel, F.; Wolter, S.; Xie, Z.; Plötz, P.-A.; Kühn, O.; Würthner, F. Biphasic Self-Assembly Pathways and Size-Dependent Photophysical Properties of Perylene Bisimide Dye Aggregates. *J. Am. Chem. Soc.* **2013**, *135*, 18722−18725.

(6) Ogi, S.; Sugiyasu, K.; Manna, S.; Samitsu, S.; Takeuchi, M. Living Supramolecular Polymerization Realized through a Biomimetic Approach. *Nat. Chem.* **2014**, *6*, 188−195.

(7) Tidhar, Y.; Weissman, H.; Tworowski, D.; Rybtchinski, B. Mechanism of Crystalline Self-Assembly in Aqueous Medium: A Combined Cryo-TEM/Kinetic Study. *Chem.—Eur. J.* **2014**, *20*, 10332−10342.

(8) Jonkheijm, P.; van der Schoot, P.; Schenning, A. P. H. J.; Meijer, E. W. Probing the Solvent-Assisted Nucleation Pathway in Chemical Self-Assembly. *Science* **2006**, *313*, 80−83.

(9) Würthner, F. Perylene Bisimide Dyes as Versatile Building Blocks for Functional Supramolecular Architectures. *Chem. Commun.* **2004**, 1564−1579.

(10) Seibt, J.; Marquetand, P.; Engel, V.; Chen, Z.; Dehm, V.; Würthner, F. On the Geometry Dependence of Molecular Dimer Spectra with an Application to Aggregates of Perylene Bisimide. *Chem. Phys.* **2006**, *328*, 354−362.

(11) Fink, R. F.; Seibt, J.; Engel, V.; Renz, M.; Kaupp, M.; Lochbrunner, S.; Zhao, H.-M.; Pfister, J.; Würthner, F.; Engels, B. Exciton Trapping in π-Conjugated Materials: A Quantum-Chemistry-Based Protocol Applied to Perylene Bisimide Dye Aggregates. *J. Am. Chem. Soc.* **2008**, *130*, 12858−12859.

(12) Seibt, J.; Winkler, T.; Renziehausen, K.; Dehm, V.; Würthner, F.; Meyer, H.-D.; Engel, V. Vibronic Transitions and Quantum Dynamics in Molecular Oligomers: A Theoretical Analysis with an Application to Aggregates of Perylene Bisimides. *J. Phys. Chem. A* **2009**, *113*, 13475−13482.

(13) Shao, C.; Grüne, M.; Stolte, M.; Würthner, F. Perylene Bisimide Dimer Aggregates: Fundamental Insights into Self-Assembly by NMR and UV/Vis Spectroscopy. *Chem.—Eur. J.* **2012**, *18*, 13665−13677.

(14) Hunter, C. A. The Role of Aromatic Interactions in Molecular Recognition. *Chem. Soc. Rev.* **1994**, *23*, 101−109.

(15) Chen, Z.; Fimmel, B.; Würthner, F. Solvent and Substituent Effects on Aggregation Constants of Perylene Bisimide π-Stacks − A Linear Free Energy Relationship Analysis. *Org. Biomol. Chem.* **2012**, *10*, 5845−5855.

(16) Sadrai, M.; Hadel, L.; Sauers, R. R.; Husain, S.; Krogh-Jespersen, K.; Westbrook, J. D.; Bird, G. R. Lasing Action in a Family of Perylene Derivatives: Singlet Absorption and Emission Spectra, Triplet Absorption and Oxygen Quenching Constants, and Molecular Mechanics and Semiempirical Molecular Orbital Calculations. *J. Phys. Chem.* **1992**, *96*, 7988−7996.

(17) Kasha, M.; Rawls, H. R.; El-Bayoumi, M. A. The Exciton Model in Molecular Spectroscopy. *Pure Appl. Chem.* **1965**, *11*, 371−392.

(18) Chen, Z.; Stepanenko, V.; Dehm, V.; Prins, P.; Siebbeles, L. D. A.; Seibt, J.; Marquetand, P.; Engel, V.; Würthner, F. Photoluminescence and Conductivity of Self-Assembled π−π Stacks of Perylene Bisimide Dyes. *Chem.—Eur. J.* **2007**, *13*, 436−449.

(19) May, V.; Kühn, O. *Charge and Energy Transfer Dynamics in Molecular Systems*; Wiley-VCH: Berlin, 2000.

(20) Fulton, R. L.; Goutermann, M. Vibronic Coupling. II. Spectra of Dimers. *J. Chem. Phys.* **1964**, *41*, 2280−2286.

(21) Lim, J. M.; Kim, P.; Yoon, M.-C.; Sung, J.; Dehm, V.; Chen, Z.; Würthner, F.; Kim, D. Exciton Delocalization and Dynamics in Helical π-Stacks of Self-Assembled Perylene Bisimides. *Chem. Sci.* **2013**, *4*, 388−397.

(22) Due to a charge-transfer character between the electron-rich imide substituents and the electron-deficient PBI core, **1** shows moderate positive solvatochromism (Supporting Information Figure S4), rendering the monomer fluorescence lifetime strongly dependent on solvent polarity (1.6 ns in $CHCl_3$/MCH, 3.5 ns in pure MCH).

(23) Yatskou, M. M.; Donker, H.; Novikov, E. G.; Koehorst, R. B. M.; van Hoek, A.; Apanasovich, V. V.; Schaafsma, T. J. Nonisotropic Excitation Energy Transport in Organized Molecular Systems: Monte Carlo Simulation-Based Analysis of Fluorsecence and Fluorescence Anisotropy Decay. *J. Phys. Chem. A* **2001**, *105*, 9498−9508.
(24) Yatskou, M. M.; Koehorst, R. B. M.; van Hoek, A.; Donker, H.; Schaafsma, T. J.; Gobets, B.; van Stokkum, I.; van Grondelle, R. Spectroscopic Properties of a Self-Assembled Zinc Porphyrin Tetramer II. Time-Resolved Fluorescence Spectroscopy. *J. Phys. Chem. A* **2001**, *105*, 11432−11440.
(25) Lakowicz, J. R. *Principles of Fluorescence Spectroscopy*; Springer: New York, 2006.
(26) Gao, F.; Zhao, Y.; Liang, W. Z. Vibronic Spectra of Perylene Bisimide Oligomers: Effects of Intermolecular Charge-Transfer Excitation and Conformational Flexibility. *J. Phys. Chem. B* **2011**, *115*, 2699−2708.
(27) Schubert, A.; Settels, V.; Liu, W.; Würthner, F.; Meier, C.; Fink, R. F.; Schindlbeck, S.; Lochbrunner, S.; Engels, B.; Engel, V. Ultrafast Exciton Self-Trapping upon Geometry Deformation in Perylene-Based Molecular Aggregates. *J. Phys. Chem. Lett.* **2013**, *4*, 792−796.
(28) Katoh, R.; Sinha, S.; Murata, S.; Tachiya, M. Origin of the Stabilization Energy of Perylene Excimer as Studied by Fluorescence and Near-IR Transient Absorption Spectroscopy. *J. Photochem. Photobiol., A* **2001**, *145*, 23−34.
(29) Katoh, R.; Katoh, E.; Nakashima, N.; Yuuki, M.; Kotani, M. Near-IR Absorption Spectrum of Aromatic Excimers. *J. Phys. Chem. A* **1997**, *101*, 7725−7728.
(30) Brown, K. E.; Salamant, W. A.; Shoer, L. E.; Young, R. M.; Wasielewski, M. R. Direct Observation of Ultrafast Excimer Formation in Covalent Perylenediimide Dimers Using Near-Infrared Transient Absorption Spectroscopy. *J. Phys. Chem. Lett.* **2014**, *5*, 2588−2593.
(31) Bradforth, S. E.; Jimenez, R.; van Mourik, F.; van Grondelle, R.; Fleming, G. R. Excitation Transfer in the Core Light-Harvesting Complex (LH-1) of *Rhodobacter sphaeroides*: An Ultrafast Fluorescence Depolarization and Annihilation Study. *J. Phys. Chem.* **1995**, *99*, 16179−16191.
(32) Jimenez, R.; Dikschit, S. N.; Bradforth, S. E.; Fleming, G. R. Electronic Excitation Transfer in the LH2 Complex of *Rhodobacter sphaeroides*. *J. Phys. Chem.* **1996**, *100*, 6825−6834.
(33) Ahrens, M. J.; Sinks, L. E.; Rybtchinski, B.; Liu, W.; Jones, B. A.; Giaimo, J. M.; Gusev, A. V.; Goshe, A. J.; Tiede, D. M.; Wasielewski, M. R. Self-Assembly of Supramolecular Light-Harvesting Arrays from Covalent Multi-Chromophore Perylene-3,4:9,10-bis(dicarboximide) Building Blocks. *J. Am. Chem. Soc.* **2004**, *126*, 8284−8294.